Volume 18, Number 3, 2025. pp. 375-388

Jordan Journal of Physics

ARTICLE

Natural Radioactivity and Estimation of Radiation Doses in Some Northern Jordanian Buildings

Talal S. M. Haimur[a], **Saleh R. Al-Bashaish**[a] and **Marwan S. Mousa**[b]

[a] *Department of Allied Sciences, Faculty of Arts and Sciences, Al-Ahliyya Amman University, P.O. Box 19328 Amman, Jordan.*

[b] *Department of Renewable Energy Engineering, Jadara University, Irbid 21110, Jordan.*

Doi: **https://doi.org/10.47011/18.3.10**

Received on: 27/03/2024; *Accepted on: 03/09/2024*

Abstract: The radioactivity of different types of building materials used in Jordan was analyzed using a high-purity germanium detector (HPGe). The measured activity concentrations of ^{238}U, ^{235}U, ^{232}Th, ^{226}Ra, and ^{40}K in $Bq.kg^{-1}$ were found in ranges of 1.7-66.1, 0.02-1.7, 0.3-11, 1.22-65.8, and 8.1-69.4, respectively. The radium equivalent activity (R_{eq}) ranged from 87.36 to 3.46 $Bq.kg^{-1}$. Mean values of the radium equivalent activity, hazard indices, absorbed dose rate, and annual effective dose were calculated. The results obtained in this investigation were analyzed and compared with data reported from other countries. With one exception, the findings are consistent with the recommended limits of the International Commission on Radiological Protection.

Keywords: Natural radioactivity, Building materials, Gamma-ray spectroscopy, Jordan, Hazard indexes.

1. Introduction

The radiological hazards of construction materials used in buildings due to the presence of natural radioactivity have been extensively investigated over the past 45 years. Several studies have been carried out to estimate the radiological hazards and annual dose contributions of natural radioactivity in buildings [1], both in Jordan and worldwide. Since people spend nearly 80% of their lives indoors [2], understanding the accumulation of radioactive nuclei in construction components is crucial for evaluating radiation exposure. Among the different radio-nuclides, $^{40}K_{19}$ and members of the natural radioactive series starting with $^{238}U_{92}$, $^{235}U_{92}$, and $^{232}Th_{90}$, are to be considered [3]. These radionuclides are found geologically in soils and hard rocks and are widely distributed in the environment [4]. Building materials derived from such ores and raw resources inevitably contain varying levels of these radionuclides, thereby increasing the absorbed dose of residents through external exposure [5, 6]. The γ-rays, as has been largely recognized, can seriously cause a great deal of damage to the human body [7]. High radium exposure could cause immune suppression, anemia, cataracts, and tooth frailty. These health impacts are realized only through extreme exposure to radium in the workplace [3]. Health risks might exist in many forms: accumulation of the radio-nuclide dust through mining, aggregation in the kidneys and bones, or cancer [8]. For this reason, there is a growing need to control the use of soil-derived materials, such as cement, ceramic, granite, and decorative stones. These materials can serve as an additional source of radiation exposure to people [9].

In this study, gamma radiation measurements are reported for a variety of naturally occurring rocks in Jordan, marketed under different commercial names. These results are of general interest since such rocks are globally used as building and ornamental materials. A standard

Corresponding Author: Talal S. M. Haimur **Email**: thaimur@ammanu.edu.jo

high-purity germanium detector was used for these measurements, but advanced gamma detection systems that use high-resolution, coincidence/anti-coincidence, and thorough background analyses to suppress background and detect weak radionuclides can also be useful for studies of radiological hazards [10-14].

2. Materials and Methods

2.1. Sample Collection

Thirty-one samples of different types of construction components used in the northern area of Jordan were collected. It was noted that some construction materials are directly used in construction, primarily hard limestone. These materials are usually uprooted and drawn as they are, and then taken directly for uses in building construction, a fact that is confirmed in the natural formation of this type of building material. In this study, ten samples (group 1) were taken from these materials and then cut into parallel slices of known thickness to fit the detector system. The characteristics of these natural construction materials are presented in Table 6.

Materials of the second type have been processed in the laboratory as a concrete mixture (cement, aggregate, sand, and water). These materials have been prepared and processed manually in the laboratory. Five concrete mixtures (group 2), equipped with specific components, were packed and sealed using polyethylene Marinelli beakers and stored to dry for twelve hours and then dipped in water for a period of thirty-six hours. Then the samples were put under the sunlight to dry naturally for five days. The details of these processed samples are given in Table 7.

Finally, the third type included factory-processed construction materials: six tiles (group 3), five bricks (group 4), and five ceramic samples (group 5). These materials were collected from different factories, where they were manufactured and equipped for use as building materials. Their compositions and manufacturing methods were used to characterize these man-made products. The specifications of these samples are summarized in Table 8.

Samples under investigation were put in sealed plastic bags for one month before starting the process of measuring the radioactivity contents of these samples within the device (high-pure germanium detector and computer system), in order to assess the status of internal stability between ^{226}Ra and ^{231}Th and their progeny.

2.2. Spectroscopic Analysis

The activity concentrations of natural radionuclides in the prepared samples were measured at the Radiation Measurements Laboratory, Al-Balqa Applied University, Jordan. For energy calibration and efficiency evaluation, standard reference materials (RGU-1, RGTh-1, RGK-1), certified by the International Atomic Energy Agency [15], were used.

The detection system consisted of a p-type well-type high-purity germanium detector (GWL) with a standard energy resolution of 2.09 keV and a relative efficiency of 56.9% at 1.33 MeV of ^{60}Co. The detector was cylindrical, with dimensions of 3 inches in diameter and 3 inches in thickness, made of 99.99999998% pure germanium crystal. To minimize background radiation, the detector was surrounded by a 15-cm-thick lead shield. The shield was mounted directly on a liquid nitrogen cylinder, which cooled the detector to the operating temperature of liquid nitrogen (77 ^{40}K). The software, Gamma Vision (Model A66-B32, Version 5 [16], has been readily supplied with the detector system. Absolute errors in the measured values were estimated, based upon the Gaussian distribution, using the uncertainty in the number of counts given by the software [7]. Gamma ray spectra were analyzed for photo peaks of uranium, thorium daughter products, and ^{40}K. The ^{226}Ra radio-nuclide level has been estimated from photo peaks of ^{214}Pb at 295.22 keV (19.30%), 351.93 keV (37.6%), photo peaks of ^{214}Bi at 609.31 keV (46.1%), and 1764.49 keV (15.4%), and photo peaks of ^{234}Pa at 1001.3 keV (0.838%), and 766.36 keV (0.317%). Similarly, ^{232}Th radio-nuclide level was estimated from photo peaks of ^{228}Ac at 911.2 keV (25.8%), 968.97 keV (15.8%), and 338.32 keV (11.27%), photo peaks of ^{208}Tl at 2614.53 keV (35.64%), 583.19 keV (30.72%), photo peaks of ^{212}Bi at 727.33 keV (6.67%), 39.86 keV (27.7%), and the 238.6 keV (43.6%) photo peak of ^{212}Pb. Finally, the ^{40}K radio-nuclide level was measured directly using the (1460.72 keV) (10.7%) gamma photo peak.

2.3. The Design of Detector Shielding

The purpose of detector shielding is to reduce the amount of radiation from background sources reaching the detector. This background derives from radioactive nuclides within the environment, primarily ^{40}K in natural potassium and the uranium decay chain nuclides. Adequate reduction in the external gamma radiation intensity is not the only criterion that must be considered. As the atomic number of an absorber increases, the importance of Compton scattering as the primary interaction decreases relative to photoelectric absorption and pair production. If a shield is made of lead rather than iron, fewer gamma-rays will be Compton scattered as opposed to being absorbed. That, in turn, means that there will be fewer scattered gamma-rays to penetrate the shielding from outside and, perhaps more importantly, fewer backscattered gamma-rays from within the shield. Conventionally, detector shielding consists of 100 mm of lead. Although a greater thickness of lead would provide a greater reduction in background peak heights, the greater mass of lead available for interaction with cosmic rays would lead to an increase in the overall background continuum level. Therefore, 100-150 mm of lead is regarded as optimum. The detector is mounted within a thin aluminum retaining sleeve, which also serves as the outer contact with the detector. The core contact is made with either a conical pin or a spring-loaded pin extending within the hollow core. This arrangement is fixed to a pedestal, which is connected to the copper cold finger extending through the cryostat to the liquid nitrogen reservoir. The complete assembly is then covered by the end cap to form a sealed chamber. The upper part of the detector housing is evacuated and thermally insulated from the rest of the housing. A pack of charcoal or molecular sieve absorbent is mounted in the detector chamber to absorb traces of gases left after evacuation when the detector is cooled. Beneath the detector pedestal, preamplifier field-effect transistors (FETs) are secured and cooled for stable operation [17].

Figures 1-3 show the electronic structure of the high-purity germanium detector and the liquid nitrogen reservoir.

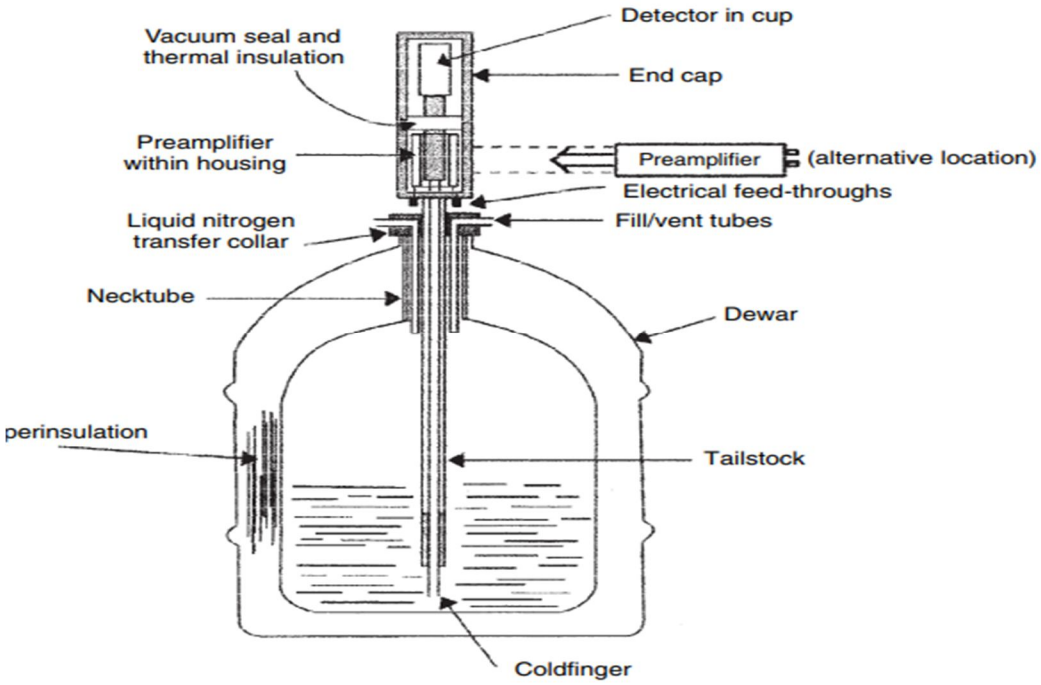

FIG. 1. A typical germanium detector, including the cryostat and liquid nitrogen reservoir.

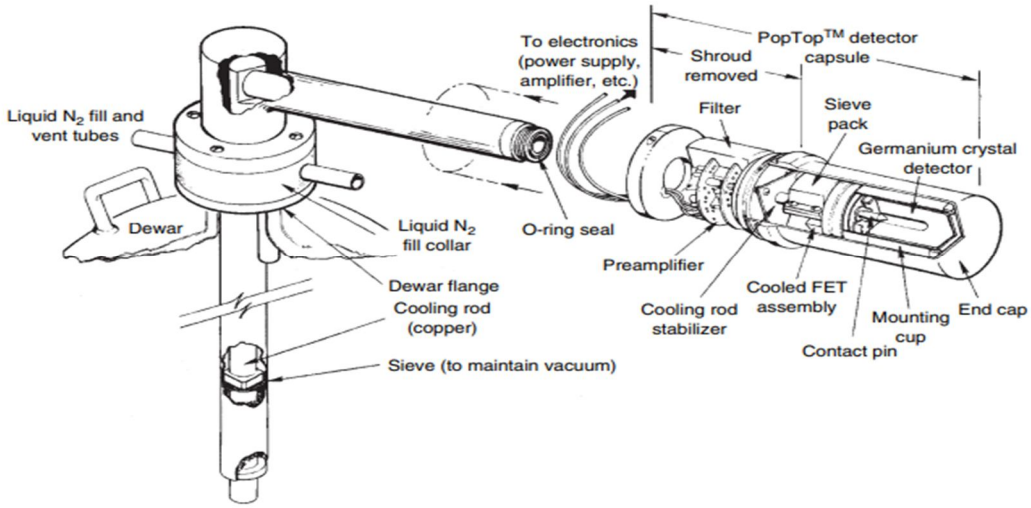

FIG. 2. A modern arrangement of detector and preamplifier within the cryostat housing – an exploded view of the ORTEC Pop-Top™ detector capsule with a horizontal dipstick cryostat and a 20 l Dewar. Reproduced by permission of ORTEC.

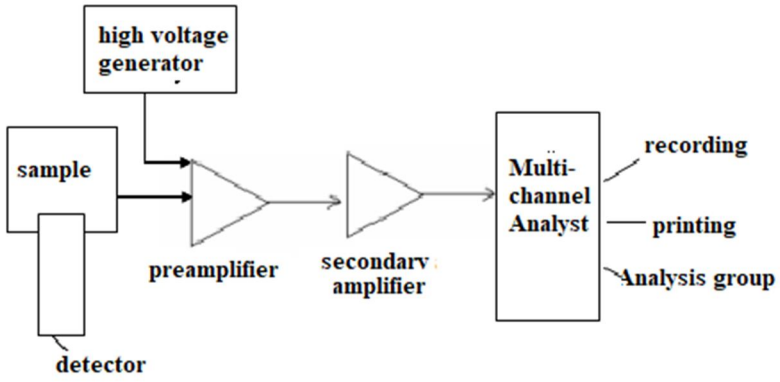

FIG. 3. Electronic structure of a high-purity germanium detector

3. Calculations

3.1 Radioactive Nuclei Accumulation

The calculations of the activity concentration (A_{Ei}) values of ^{235}U, ^{238}U, ^{232}Th series, and ^{40}K in the samples were carried out by using the following equation [18]:

$$A_{Ei} = N_{Ei} / (\varepsilon_E)\,(t)\,(\gamma_d)\,(m) \qquad (1)$$

where A_{Ei} represents the nucleus i-activity at energy Ei, N_{Ei} represents the number of peak photos at energy Ei, ϵ_E is the detection efficiency of energy Ei, t represents the counting time, γ_d represents the gamma emission resulting from each disintegration at the energy Ei of this nucleus, and m represents the mass sample in kg.

The determination of $^{238}U_{90}$ was performed indirectly through its gamma-emitting daughter nuclides, assuming that they exist in secular equilibrium with their precursors [18]. The contribution of ^{226}Ra at the energy peak (186.21 keV) can be calculated from ^{214}Pb at the energy line (295.2 keV).

The $^{235}U_{90}$ activity in building materials is rarely reported due to difficulties in gamma-ray spectrometry. The only usable photopeak for ^{235}U is at 185.72 keV [18, 19], which is recorded in the same region as the peak of ^{226}Ra (186.21 keV, 3.59%).

3.2. Radium Equivalent Activity (Ra_{eq})

Due to the irregular distributions of radionuclides ^{226}Ra, ^{232}Th, and ^{40}K in samples under investigation, it is possible to calculate the radium equivalent activity (Ra_{eq}), which is defined according to the estimation that 1 $Bq.kg^{-1}$ of ^{226}Ra, 0.7 $Bq.kg^{-1}$ of ^{232}Th, and 13$Bq.kg^{-1}$ of ^{40}K produce the same gamma ray dose [20-22, 1]:

$$Ra_{eq} = A(Ra) + 1.43\,A(Th) + 0.077\,A(K) \qquad (2)$$

where A(Ra), A(Th), and A(K) are the specific activities of ^{226}Ra, ^{232}Th and ^{40}K in $Bq.kg^{-1}$, respectively. The maximum value of Ra_{eq} in building constructions must be less than 370 for safe use [23].

3.3. Hazard Indices

To consider radiological hazards from building materials as negligible, the external and internal gamma radiation doses should be limited to 1mSvy^{-1}. Thus, we can calculate the external and internal hazard indices when the safety requirements for building structures are being satisfied. Hence, the external dose should not exceed 1.5 mSv. y^{-1} [23].

For samples under investigation, the external hazard index (H_{ex}) and the internal hazard index (H_{in}) can be calculated by using the following equations [4, 19, 21, 22]:

$$H_{ex} = A(^{226}Ra)/370 + A(^{223}Th)/259 + A(^{40}K)/4810 \leq 1 \quad (3)$$

$$H_{in} = A(^{226}Ra)/185 + A(^{232}Th)/259 + A(^{40}K)/4810 \leq 1 \quad (4)$$

where $A(^{226}Ra)$, $A(^{90}Th)$, and $A(^{40}K)$ are the specific activities of ^{226}Ra, ^{232}Th, and ^{40}K, respectively.

3.4. Estimation of Gamma Absorbed Dose Rate (D)

The conversion factor used for calculating the absorbed gamma dose rate D (in nGy·h^{-1}) corresponds to 0.92 nGy·h^{-1} per Bq·kg^{-1} for ^{226}Ra, 1.1 nGy·h^{-1} per 1 Bq·kg^{-1} for ^{232}Th, and 0.08 nGy·h^{-1} per 1 Bq·kg^{-1} for ^{40}K. For samples under investigation, it is possible to calculate (D) by using the equation [1, 24, 25]:

$$D\ (nGy.\ h^{-1}) = 0.08\ A(K_{19}) + 0.092A(Ra_{88}) + 1.1\ A(Th_{90}) \quad (5)$$

Here, $A(K_{19})$, $A(Ra_{88})$, and $A(Th_{90})$ are specific activities (in Bq.kg^{-1}) of $^{40}K_{19}$, $^{226}Ra_{88}$, and $^{232}Th_{90}$, respectively.

3.5. Annual Effective Absorbed Dose (AED)

The annual effective absorbed dose (H_E) in mSv.y^{-1} can be calculated by the formula [4, 21]:

$$H_E\ (mSv.y^{-1}) = D(nGy.h^{-1}) \times T \times F \quad (6)$$

where T is the indoor occupancy time, which is approximately 80% of the year (8760 hy^{-1}), and F is the gamma conversion factor (0.7×10^{-6} SvGy^{-1}).

4. Results and Discussion

4.1. Activity Concentrations of ^{238}U, ^{35}U, ^{232}Th, ^{226}Ra, and ^{40}K

The specific activity concentrations of ^{238}U, ^{35}U, ^{232}Th, ^{226}Ra, and ^{40}K in the collected samples, including associated uncertainties (Bq.kg^{-1}), are listed in Table 1. Figure 4 illustrates the average radioactive nuclei accumulation for ^{232}Th, ^{226}Ra, and ^{40}K in the investigated construction materials used in Jordan.

The maximum activity concentrations for ^{238}U were 65.9±2.21 Bq/kg in the tile sample 3-T6, and the minimum was 1.7 ± 0.05 Bq/kg in brick sample 4-B1. For ^{235}U, the maximum concentration was 1.72 ± 0.01 in sample 4-B4, and the minimum concentration was 0.03±0.01 in ceramic sample 5-Cc1. For ^{232}Th, the maximum concentration was 11.00 ± 4.41 Bq/kg in ceramic sample 5-Cc3, while the minimum concentration was 0.30±0.01 Bq/kg in brick sample 4-B2. For ^{226}Ra, the maximum concentration was 66.10±2.31 Bq/kg in tile sample 3-T6, while the minimum concentration was 1.03±0.04 Bq/kg in brick sample 4-B1. For ^{40}K, the maximum concentration was 692.10±16.90 Bq/kg in ceramic sample 5-Cc4, while the minimum was 9.10±1.21 Bq/kg in brick sample 4-B4.

From these results, it can be seen that the building materials of type three (factory-processed materials, group (B), bricks) have the minimum average concentrations among all material types. Additionally, we found that specific activity concentration due to ^{40}K contributed the most to the total radioactivity for all samples (Figure 4). In general, the average activity concentrations of natural radionuclides in all samples were below the world averages of 50 Bq.kg^{-1} for ^{226}Ra and ^{232}Th, and 500 Bq.kg^{-1} for ^{40}K [27], except for four samples: ^{226}Ra in tile sample 3-T6 that reached 66.10 ± 2.31 Bq/kg and ^{40}K in ceramic samples 5-Cc3, 5-Cc4, and 5-Cc5 that reached 518.80± 22.20, 692.10± 16.90, and 536.5 0± 9.61, respectively.

TABLE 1. The radioactive nuclei accumulation measured for samples under investigation on average (in Bq kg-^{1}).

Sample code	^{238}U	^{235}U	^{232}Th	^{226}Ra	^{40}K
1-R1(stone)	10.29 ± 1.18	0.16 ± 0.08	5.90 ± 1.61	10.20 ± 1.31	120.90 ± 9.21
1-R2(stone)	07.10 ± 0.80	0.30 ± 0.07	1.00 ± 0.00	06.98 ± 1.92	031.80 ± 6.32
1-R3(stone)	04.00 ± 0.68	0.10 ± 0.05	2.19 ± 1.11	04.00 ± 0.81	032.90 ± 5.70
1-R4(stone)	11.50 ± 0.85	0.10 ± 0.06	4.10 ± 3.01	11.20 ± 0.91	073.10 ± 6.33
1-R5(stone)	12.50 ± 1.00	0.14 ± 0.06	7.40 ± 4.22	12.40 ± 1.20	084.90 ± 15.80
1-R6(stone)	14.50 ± 1.39	0.13 ± 0.09	1.40 ± 0.71	14.40 ± 1.51	064.00 ± 6.21
1-R7(stone)	10.10 ± 2.70	0.40 ± 0.11	1.20 ± 0.70	09.70 ± 2.92	036.80 ± 3.11
1-R8(stone)	09.40 ± 3.58	0.51 ± 0.21	1.20 ± 1.00	08.90 ± 3.90	033.70 ± 1.83
1-R9(stone)	16.30 ± 1.20	0.20 ± 0.08	8.50 ± 2.32	16.20 ± 1.22	047.00 ± 9.31
1-R10(stone)	19.00 ± 0.10	0.10 ± 0.01	10.10 ± 3.21	19.00 ± 0.05	050.00 ± 8.91
2-Ct1(cement)	10.90 ± 3.22	0.20 ± 0.11	5.70 ± 1.41	10.70 ± 1.81	220.00 ± 17.04
2-Ct2(cement)	12.00 ± 1.21	0.13 ± 0.08	6.40 ± 1.21	11.80 ± 1.32	128.70± 14.22
2-Ct3(cement)	13.50 ± 0.31	0.05 ± 0.03	7.90 ± 1.71	13.50 ± 0.41	400.00 ± 18.90
2-Ct4(cement)	13.10 ± 1.51	0.12 ± 0.01	7.00 ± 2.20	13.00 ± 1.60	268.70± 16.41
2-Ct5(cement)	10.47 ± 1.72	0.31 ± 0.02	5.00 ± 0.51	10.20 ± 1.81	223.80± 17.22
3-T1(cement)	14.80 ± 0.12	0.10 ± 0.01	1.00 ± 0.30	14.70 ± 0.12	212.00 ± 18.82
3-T2(tile)	24.90 ± 0.31	0.10 ± 0.01	5.50 ± 3.60	25.00 ± 0.41	214.60± 15.91
3-T3(tile)	33.40 ± 0.59	0.10 ± 0.04	0.90 ± 0.10	33.40 ± 0.70	133.50± 17.63
3-T4(tile)	15.40 ± 0.51	0.10 ± 0.02	1.00 ± 0.15	15.40 ± 0.52	148.00 ± 17.68
3-T5(tile)	14.50 ± 0.62	0.02 ± 0.00	1.00 ± 0.20	14.50 ± 0.61	201.00 ± 13.88
3-T6(tile)	65.90 ± 2.21	0.32 ± 0.01	1.20 ± 0.20	66.10 ± 2.31	259.10± 12.52
4-B1(brick)	01.70 ± 0.05	0.65 ± 0.01	0.50 ± 0.10	01.03 ± 0.04	022.40 ± 3.51
4-B2(brick)	05.10 ± 0.51	0.70 ± 0.03	0.31 ± 0.01	04.40 ± 0.51	043.40 ± 4.71
4-B3(brick)	08.30 ± 1.92	1.62 ± 0.11	0.40 ± 0.10	06.70 ± 3.42	029.60 ± 1.93
4-B4(brick)	05.10 ± 1.17	1.72 ± 0.01	0.45 ± 0.21	03.40 ± 1.28	009.10 ± 1.21
4-B5(brick)	05.02 ± 1.14	1.18 ± 0.01	0.40 ± 0.10	03.81 ± 0.60	025.71 ± 1.70
5-Cc1(ceramic)	08.70 ± 0.21	0.03 ± 0.01	0.62 ± 0.20	08.70 ± 0.11	209.70 ± 19.01
5-Cc2(ceramic)	06.50 ± 0.28	0.40 ± 0.03	6.10 ± 0.31	06.10 ± 0.22	313.20 ± 32.02
5-Cc3(ceramic)	26.80 ± 1.20	0.40 ± 0.08	11.00 ± 4.41	26.40 ± 1.89	518.80± 22.20
5-Cc4(ceramic)	22.30 ± 0.31	0.40 ± 0.02	4.20 ± 1.22	22.00 ± 0.31	692.10± 16.90
5-Cc5(ceramic)	26.50 ± 0.62	0.33 ± 0.03	5.50 ± 2.91	26.20 ± 0.62	536.5 0± 9.61

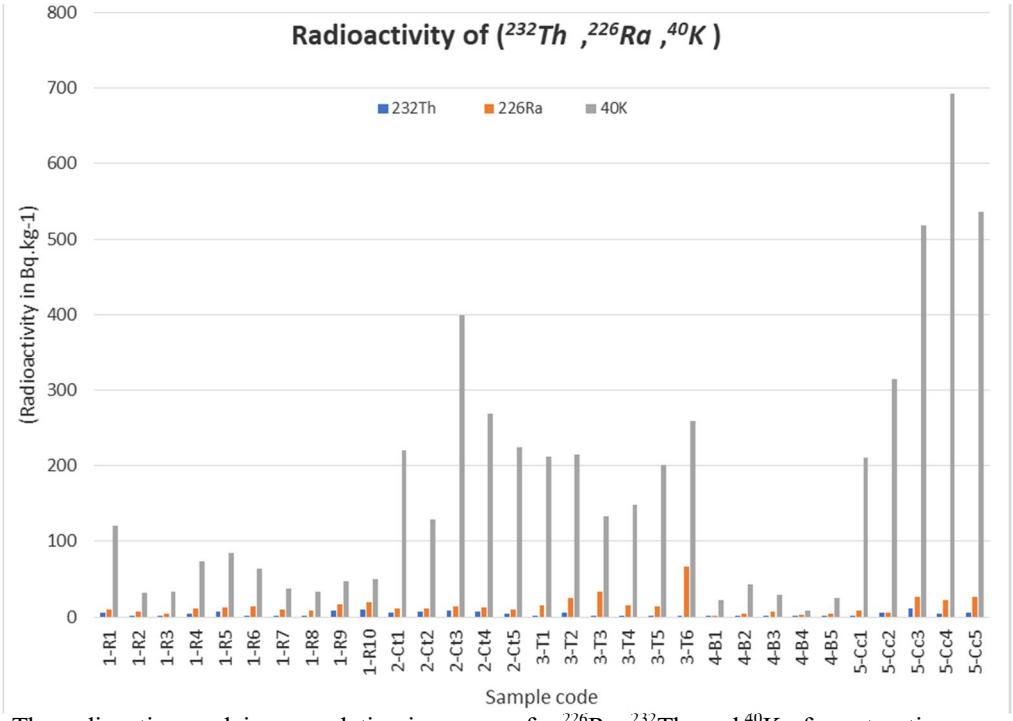

FIG. 4. The radioactive nuclei accumulation in average for ^{226}Ra, ^{232}Th, and ^{40}K of construction components used in Jordan.

4.2. Radium Equivalent Activity (Ra_{eq} in $Bq.kg^{-1}$) and Hazard Indices

The calculated values of radium equivalent (**Ra_{eq}**), external and internal hazard indices (H_{ex}, H_{in}), absorbed dose rate, and effective dose (D, HE) for all samples are summarized in Table 2. The range of radium equivalent activity from a maximum of 87.359 $Bq.kg^{-1}$ for tile sample 3-T6 to a minimum of 3.4598 $Bq.kg^{-1}$ for brick sample 4-B1 has been illustrated in Fig. 5. All samples exhibited Ra_{eq} values below the recommended upper limit of 370 $Bq.kg^{-1}$ for safe use in building materials. Hazard indices ranged from a maximum of 0.2925 for ceramic sample 5-Cc3 to a minimum of 0.0126 4-B for brick sample. The recorded absorbed dose rate presents a range from a maximum of 82.4840 $nGy\ h^{-1}$ for tile sample 3-T6 to a minimum of 3.28040 $nGy\ h^{-1}$ for brick sample. The effective dose ranges from a maximum of 0.4046 $mSvy^{-1}$ for the tile sample to 0.0161 $mSvy^{-1}$ for brick sample 4-B1. All values are below the recommended average indoor dose rate of 84 $nGyh^{-1}$ suggested for construction materials [23], indicating negligible radiological risk for humans, whether at home or in the workplace [36].

TABLE 2. Radium equivalent, external and internal hazard indexes, absorbed dose rate, and effective dose of absorption per year calculated for all samples.

Sample code	Ra_{eq} *($Bq.kg^{-1}$)*	H_{ex}	H_{in}	*D ($nGy\ h^{-1}$)*	*HE ($mSvy^{-1}$)*
1-R1(stone)	27.954	0.0754	0.1031	25.5540	0.1254
1-R2(stone)	10.894	0.0294	0.0484	10.1000	0.0496
1-R3(stone)	09.687	0.0261	0.0370	08.7400	0.0429
1-R4(stone)	22.684	0.0612	0.0916	20.6540	0.1013
1-R5(stone)	29.527	0.0797	0.1132	26.3480	0.1293
1-R6(stone)	21.330	0.0576	0.0966	19.9080	0.0977
1-R7(stone)	14.188	0.0383	0.0646	13.1240	0.0644
1-R8(stone)	13.234	0.0357	0.0598	12.2280	0.0600
1-R9(stone)	31.974	0.0863	0.1302	28.0140	0.1374
1-R10(stone)	37.293	0.1006	0.1521	32.5900	0.1599
2-Ct1(cement)	35.791	0.0966	0.1256	33.7140	0.1654
2-Ct2(cement)	30.885	0.0833	0.1153	28.2160	0.1384
2-Ct3(cement)	55.597	0.1500	0.1866	53.1100	0.2605
2-Ct4(cement)	43.723	0.1180	0.1532	41.1800	0.2020
2-Ct5(cement)	34.598	0.0934	0.1210	32.8040	0.1609
3-T1(cement)	32.454	0.0877	0.1274	31.5840	0.1549
3-T2(tile)	49.42	0.1334	0.2011	46.2500	0.2269
3-T3(tile)	45.082	0.1218	0.2121	42.5180	0.2086
3-T4(tile)	28.226	0.0762	0.1179	27.1080	0.1330
3-T5(tile)	31.407	0.0848	0.1240	30.5200	0.1497
3-T6(tile)	87.359	0.2360	0.4136	82.4840	0.4046
4-B1(brick)	3.4598	0.0093	0.0121	3.28040	0.0161
4-B2(brick)	8.1708	0.0221	0.0340	07.8500	0.0385
4-B3(brick)	9.5512	0.0258	0.0439	08.9720	0.0440
4-B4(brick)	4.6672	0.0126	0.0218	04.2710	0.0210
4-B5(brick)	6.4211	0.0175	0.0279	06.0934	0.0298
5-Cc1(ceramic)	25.7566	0.0696	0.0931	25.4860	0.1250
5-Cc2(ceramic)	38.924	0.1050	0.12160	37.3620	0.1833
5-Cc3(ceramic)	81.862	0.2209	0.2925	77.6680	0.3810
5-Cc4(ceramic)	81.2438	0.2194	0.2789	80.1720	0.3933
5-Cc5(ceramic)	75.4602	0.2037	0.2746	73.1620	0.3589

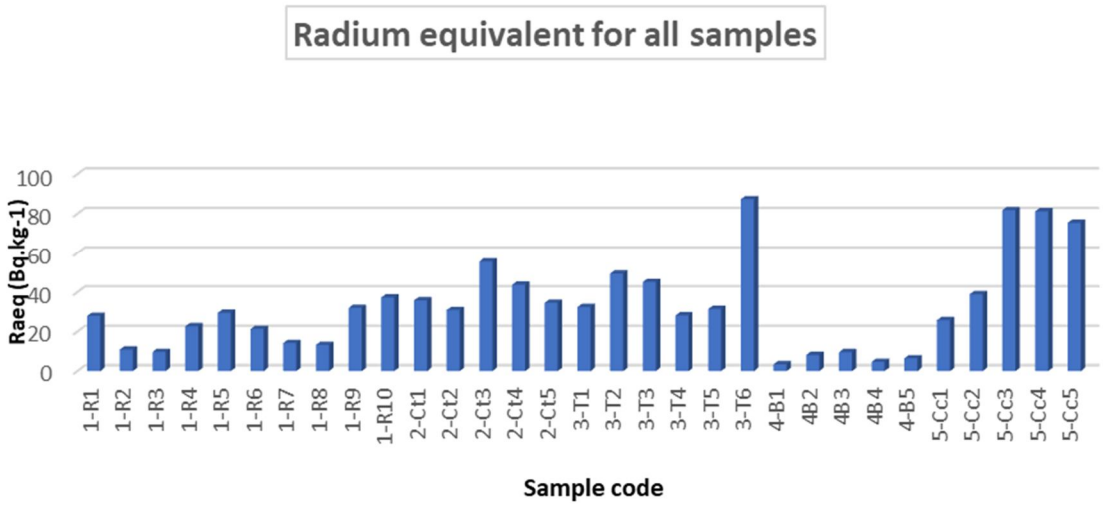

FIG. 5. Radium equivalent activity Ra_{eq} in average for the studied samples.

To compare the five studied groups—building hard rocks (stones), concrete, tiles, bricks, and ceramics—Tables 3, 4a, and 4b, along with Figs. 6–8, summarize and illustrate the results.

It is observed that the ceramics group (5-Cc) had the maximum average radium equivalent Ra_{eq} (60.64 Bq.kg^{-1}), maximum average external index H_{ex} (0.16372), maximum average internal index H_{in} (0.2121), maximum average absorbed dose rate (58.8 nGy. h^{-1}), and maximum average annual effective dose rate (0.288302 mSv. y^{-1}). The bricks group (4-B) had the minimum average radium equivalent Ra_{eq} (06.46 Bq.kg^{-1}), minimum average external index H_{ex} (0.01745), minimum average internal index H_{in} (0.02795), minimum average absorbed dose rate (06.1 nGy. h^{-1}), and minimum average annual effective dose rate (0.029892 mSv. y^{-1}).

Regarding radionuclide concentrations, the tiles group (3-T) had the highest averages for ^{226}Ra (28.12 ± 7.670 Bq kg-^{1}) and ^{238}U (28.183 ± 0.717 Bq kg-^{1}). The concrete group (2-Ct) recorded the maximum average for ^{232}Th (6.40 ± 1.40 Bq kg-^{1}), while the ceramics group (5-Cc) showed the highest average concentration of ^{40}K (453.6 ± 19.76 Bq kg-^{1}).

The bricks group (4-B), on the other hand, had the lowest average radionuclide concentrations across most isotopes: 5.05 ± 0.583333 Bq kg-^{1} for ^{238}U, 3.88 ± 1.567 Bq kg-^{1} for ^{226}Ra, 0.41 ± 0.11Bq kg-^{1} for ^{232}Th, and 25.88 ± 2.745 for ^{40}K. Ultimately, we found that it also had the highest average concentration of ^{235}U (1.1675 ± 0.035 Bq kg-^{1}).

TABLE 3. Average radiological hazard indices for radionuclides in selected building material groups under study.

Group name	Number of shambles	Average Radium equivalent activity Ra_{eq} (Bq.kg^{-1})	Average External index H_{ex}	Average Internal index H_{in}	Average Absorbed Dose Rate (nGy. h^{-1})	Average Annual Effective Dose Rate (mSv. y^{-1})
Hard rocks (stones)	10	21.88	0.02159	0.08964	19.7	0.096768
Concrete	5	40.12	0.10825	0.14035	37.8	0.185455
Tiles	6	45.67	0.12332	0.19934	43.4	0.212955
Bricks	5	06.46	0.01745	0.02795	06.1	0.029892
Ceramics	5	60.64	0.16372	0.2121	58.8	0.288302
Min		06.46	0.01745	0.02795	06.1	0.029892
Max		60.64	0.16372	0.2121	58.8	0.288302

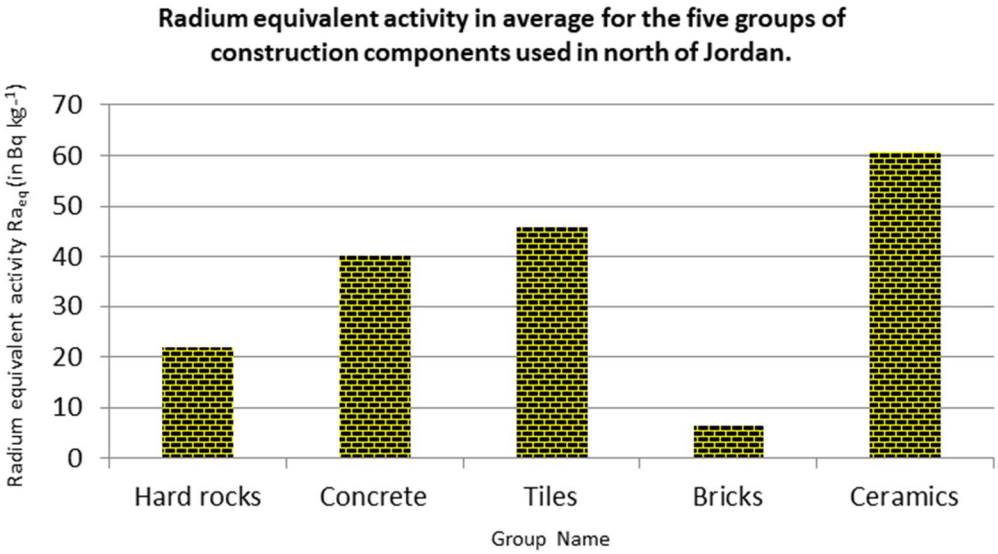

FIG. 6. Radium equivalent activity Ra_{eq} in average for the five groups of construction components used in Jordan.

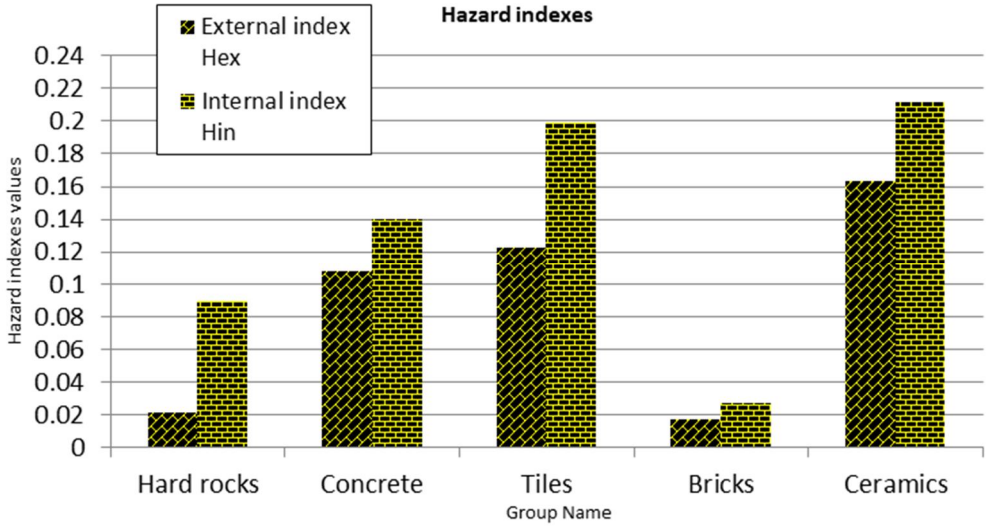

FIG. 7. Hazard indexes in average for the five groups of construction components used in Jordan.

TABLE 4a. Average activity concentrations ($Bq \cdot kg^{-1}$) of radionuclides in selected building material samples from northern Jordan, representing each group.

radionuclide	^{238}U			^{235}U		
Group name	Average activity concentration (Bq kg-1)	Minimum Average activity concentration (Bq kg-1)	Maximum Average activity concentration (Bq kg-1)	Average activity concentration (Bq kg-1)	Minimum Average activity concentration (Bq kg-1)	Maximum Average activity concentration (Bq kg-1)
Hard rocks (stones)	11.470 ± 1.350	4 ± 0.7	19 ± 0.050	0.215 ± 0.0783	0.1 ± 0.003	0.51 ± 0.200
Concrete	11.994 ± 1.580	10.47 ± 1.700	13.50 ± 0.300	0.162 ± 0.044	0.05 ± 0.020	0.31 ± 0.010
Tiles	28.183 ± 0.717	14.50 ± 0.600	66.10 ± 2.200	0.123 ± 0.020	0.02 ± 0.010	0.32 ± 0.010
Bricks	5.050 ± 0.583	1.70 ± 0.050	8.30 ± 1.900	1.1675 ± 0.035	0.65 ± 0.004	1.70 ± 0.006
Ceramics	18.160 ± 0.520	6.50 ± 0.300	26.80 ± 1.200	0.312 ± 0.032	0.03 ± 0.010	0.40 ± 0.020

TABLE 4b (continued). Average activity concentrations (Bq·kg^{-1}) of radionuclides in selected building material samples from northern Jordan, representing each group.

Radio-nuclide	^{226}Ra			^{232}Th			^{40}K		
Group name	Average activity concentration (Bq kg-$^{1)}$	Minimum Average activity concentration (Bq kg-$^{1)}$	Maximum Average activity concentration (Bq kg-$^{1)}$	Average activity concentration (Bq kg-$^{1)}$	Minimum Average activity concentration (Bq kg-$^{1)}$	Maximum Average activity concentration (Bq kg-$^{1)}$	Average activity concentration (Bq kg-$^{1)}$	Minimum Average activity concentration (Bq kg-$^{1)}$	Maximum Average activity concentration (Bq kg-$^{1)}$
Hard rocks (stones)	11.3 ± 1.565	4 ± 0.8	19 ± 0.05	4.3 ± 1.78	1 ± 0.0	10.1 ± 3.2	57.5 ± 7.26	31.8 ± 6.3	120.90 ± 9.20
Concrete	11.84 ± 1.380	10.20 ± 1.80	13.50 ± 0.40	6.40 ± 1.40	5 ± 0.5	7.9 ± 1.7	248.4 ± 16.79	128.7 ± 14.2	400 ± 18.90
Tiles	28.12 ± 7.670	14.50 ± 0.60	65.70 ± 2.30	1.77 ± 0.79	0.9 ± 0.1	5.5 ± 3.8	195 ± 16.066	133.5 ± 17.5	259.1 ± 12.50
Bricks	3.88 ± 1.567	1.02 ± 0.05	6.70 ± 4.40	0.41 ± 0.11	0.3 ± 0.02	0.5 ± 0.1	25.88 ± 2.745	8.1 ± 1.00	43.40 ± 4.70
Ceramics	17.88 ± 0.480	6.10 ± 0.20	26.40 ± 1.20	5.48 ± 1.80	0.62 ± 0.2	11 ± 4.4	453.6 ± 19.76	209.7 ± 19	691.4 ± 16.90

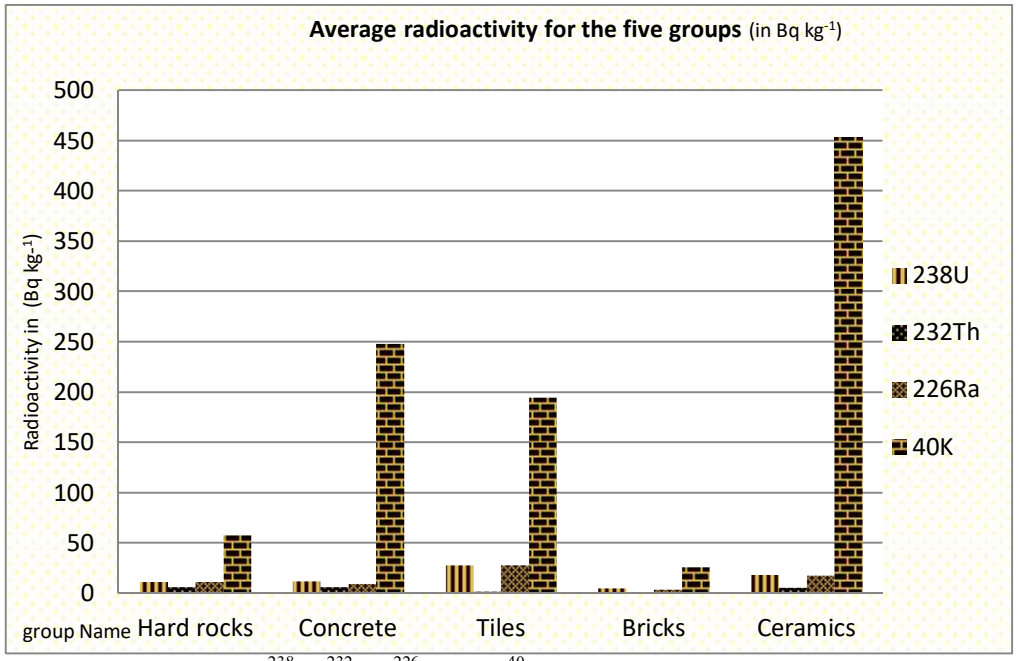

FIG. 8. Average activity concentrations of ^{238}U, ^{232}Th, ^{226}Ra, and ^{40}K in the five groups of construction components used in Jordan.

TABLE 5. Characteristics of the collected samples of natural construction materials used directly without processing.

Sample code	material	Type	Origin	Dimensions (mm)	Weight (kg)	Counting time (s)
1-R1	stone	Walls White Stone	Ajloun /Jordan	30*100*100	0.9921	92435.36
1-R2	stone	Walls Red Stone	Hayyan /Jordan	30*98*98	0.6359	88268
1-R3	stone	Walls White stone	Hayyan / Jordan	28*100*100	0.7199	252915.9
1-R4	stone	Walls White stone	Halabat / Jordan	30*100*100	0.7584	255509.8
1-R5	stone	Walls Blue stone	Halabat / Jordan	30*100*100	0.8007	84689.3
1-R6	stone	Walls White Stone	Irbid / Jordan	30*100*100	0.9921	172016.6
1-R7	stone	Walls White Stone	Irbid / Jordan	60*100*100	1.743	170597.5
1-R8	stone	Walls White Stone	Irbid / Jordan	90*100*100	2.486	343162.6
1-R9	stone	Walls White Stone	Souf / Jordan	30*100*100	0.9891	84993.9
1-R10	stone	Walls White Stone	Souf / Jordan	30*100*100	1.002	87718.7

TABLE 6. Characteristics of laboratory-processed construction material samples.

Sample code	Material	Components	Components weight (gm)	Sample weight (kg)	Counting time (s)
2-Ct1	Cement 1	Coarse aggregate	212	0.638	81580.96
		Fine aggregate	214		
		Sand (silica)	106		
		Cement	107		
		Silt clay	107		
2-Ct2	Cement 2	Coarse aggregate	229.4	0.5735	253992.40
		Fine aggregate	1147		
		Cement	114.7		
		Silt clay	114.7		
2-Ct3	Cement 3	Coarse aggregate	116.3	0.4652	88107.30
		Fine aggregate	116.3		
		Sand (silica)	116.3		
		Cement	116.3		
2-Ct4	Cement 4	Coarse aggregate	275.9	0.578	1011069.1
		Sand (silica)	100		
		Cement	100		
		Silt clay	100		
2-Ct5	Cement 5	Coarse aggregate	366.5	0.6665	67698.18
		Fine aggregate	100		
		Sand (silica)	100		
		Cement	100		

TABLE 7. Characteristics of the collected samples of factory-processed construction materials.

Sample code	Material	Type	Origin	Counting time (s)
3-T1	Tile	Floor tile	Ma'am / Jordan	84381.48
3-T2	Tile	Floor tile	Jarash/Jordan	86416.6
3-T3	Tile	Floor tile	Turkey	88672.72
3-T4	Tile	Floor tile	Irbid/Jordan	84980.62
3-T5	Tile	Floor tile	Irbid /Jordan	87614.3
3-T5	Tile	Dubaa floor tile	Dubaa /Jordan	256407.5
4-B1	Brick	Brick walls 10 cm	Jarash/Jordan	82694.5
4-B2	Brick	Brick walls 15 cm	Jarash/Jordan	76897.96
4-B3	Brick	Brick walls 20 cm	Jarash/Jordan	172387.5
4-B4	Ribs Brick	Ceiling ribs 15cm	Jarash/Jordan	352183.5
4-B1	Ribs Brick	Ceiling ribs 15cm	Jarash/Jordan	711213.5
5-Cc1	Ceramic	Floor ceramic	Egypt	168271
5-Cc2	Ceramic	International floor ceramic	Jordan	82405.73
5-Cc3	Ceramic	Diamond floor ceramic	Jordan	80978.32
5-Cc4	Ceramic	Egyptian wall ceramic	Egypt	99888.36
5-Cc5	Ceramic	International wall ceramic	Jordan	256198.9

4.3. Comparison of the Radioactivity Concentrations with Other Research

By comparing the three studies carried out in Jordan and mentioned in this work for stone samples, we noticed that $^{226}Ra_{88}$ was reported as 18.36 Bq.kg^{-1} in [9], 27.7 Bq.kg^{-1} in [27], and 11.3 Bq.kg^{-1} in the present study. This was less than the value reported from studies from Croatia [28], which was 35 Bq.kg^{-1}. For $^{232}Th_{90}$, the reported values were 2.77 Bq.kg^{-1} in [9], 5.9 Bq.kg^{-1} in [27], and 2.77 Bq.kg^{-1} in the present study, while in Slovakia it was 25.35 Bq.kg^{-1}, which was higher than in Jordan. For ^{40}K, the reported values were 32.7 in [9], 38.6 Bq.kg^{-1} in [27], and 32.7 Bq.kg^{-1} in the present study. These results are close to one another across the Jordanian studies. For ceramic samples in the present study, the average activity concentrations were 17.9 Bq.kg^{-1}, 5.5 Bq.kg^{-1}, and 453.6 Bq.kg^{-1} for ^{226}Ra, ^{232}Th, and ^{40}K, respectively. These values are generally lower than those reported in other referenced studies, with the exception of potassium, which exceeds the world average of 370 Bq.kg^{-1} [27].

For cement and brick samples, the activity concentrations were also lower than the corresponding values reported in other studies.

Overall, Table 8 demonstrates that the average activity concentrations for all studied samples are below the recommended world averages, except for ^{40}K in ceramic samples. In comparison with data from other countries, the measured activity concentrations of $^{226}Ra_{88}$, $^{232}Th_{90}$, and $^{40}K_{19}$ fall within the reported ranges, confirming consistency with international findings.

TABLE 8. Comparison of average radioactive nuclei accumulation (Bq.kg^{-1}) in selected building material samples with previous studies.

Building material	*Average Radioactivity concentration (Bq.kg^{-1})*			*Country*	*Reference*
	^{226}Ra	^{232}Th	^{40}K		
Hard rocks (Limestone)	11.3	4.3	57.5	Jordan	(present study)
Limestone	10.5	0.67	3.7	Jordan	[7,37]
Hard rock Halabat	27.7	5.9	38.6	Jordan	[27]
Stone (Hard rocks)	40.8-47.7	13.7-35.0	340.0-363.3	Jordan	[36]
Limestone	10	13.4	115	Austria	[28]
Limestone	35	7.8	57	Croatia	[28]
Stone	8-16	12-18	230-803	Bangladesh	[29]
Stone	4.98	25.35	370.06	Slovakia	[30]
Stone	18.36	2.77	32.7	Jordan	[9]
Ceramic	17.9	5.5	453.6	Jordan	(present study)
	32.6	28.3	413.5	Jordan	[7.37]
	28.7	6.2	42.3	Jordan	[27]
	140.5	101.1	570.1	Jordan	[36]
	47.4	42.84	313.6	Egypt	[31]
	38	47	697	China	[32]
	58	51	473	Italia	[33]
	73.7	58.2	624	Palestine	[34]
	71.3	86.5	522	Saudi Arabia	[5]
	17-80	10-54	207-655	Bangladesh	[29]
Cement (Concrete)	11.8	6.4	248.6	Jordan	(present study)
	9.5	4.13	29.9	Jordan	[7,36]
	38	6	138	Jordan	[27]
	43.2-49.1	11.2-13.5	11.9-265.1	Jordan	[36]
	20	13	241	Greece	[34]
	28.5	7.6	167.4	Saudi Arabia	[6]
	23	9.3	118	Austria	[28]
	59	18.9	187	Croatia	[28]
	15-34	14-24	231-426	Bangladesh	[29]
	56.65	46.65	368.58	Federal University of Gusau	[31]

Building material	*Average Radioactivity concentration (Bq.kg^{-1})*			*Country*	*Reference*
	^{226}Ra	^{232}Th	^{40}K		
Brick	3.9	0.4	25.9	Jordan	(Present study)
	6.5	1.3	6.5	Jordan	[7,37]
	35	45	710	Greece	[35]
	41	89	681	Australia	[20]
	8.7	8.6	271.2	Saudi Arabia	[6]
	7.16	46.07	705.16	Slovakia	[30]
	55.05	77.93	238.65	Federal University of Gusau	[31]

5. Conclusions

In this study, the radioactive nuclei accumulation of $^{238}U_{92}$, $^{235}U_{92}$, $^{232}Th_{90}$, $^{226}Ra_{88}$, and $^{40}K_{19}$ was measured in 31 construction material samples commonly used in northern Jordan by means of gamma-ray spectroscopy.

Measurement of the radionuclide activity of $^{238}U_{92}$, $^{235}U_{92}$, $^{232}Th_{90}$, $^{226}Ra_{88}$, and $^{40}K_{19}$ indicates that their values in the studied samples are less than the corresponding world average values, with the exception of the mean values of $^{40}K_{19}$ concentration in ceramic samples. The radium equivalent activities obtained using the concentrations of these nuclides were below the allowable level of 370 Bq/kg [20] in all studied samples. All hazard indexes are less than unity.

The quantitative results indicate that brick samples have the minimum values of radiation contents and the smallest values of dose indices, while ceramic samples have the highest. As causes of radiation hazards, most construction materials used in the northern area of Jordan can be safely considered insignificant.

References

[1] Morteza, I., Mohammademad, A., Amin, S., Ghazaleh, A., Ali, Y., Erika, K., Edit, T.-B., and Tibor, K., Environ. Sci. Pollut. Res., 28 (2021) 41492.

[2] Marlet, L. and Enn, R., Proc. Est. Acad. Sci., 61 (2012) 107.

[3] Evan, R.D., Health Phys., 17 (2) (1969) 229.

[4] Rati, V., Mahur, A., Sonkawde, R., Suhail, M.A., Azam, A., and Prasad, R., Indian J. Pure Appl. Phys., 48 (7) (2010) 473.

[5] Khan, K., Aslam, A., Orifi, S.D., and Khan, H.M., J. Environ. Radioact., 58 (1) (2002) 59.

[6] Safia, Q., Amidalddin, Alzahrani, J.H., Aamudy, Fakeha. Z., M., A., Al-Habeadi, H., and Ibrahim, N., Life Sci. J., 12 (2015).

[7] Awadallah, M.I. and Imran, M.M.A., J. Environ. Radioact., 94 (3) (2007) 129.

[8] Darby, S., Hill. D., and Doll, R., Ann. Oncol., 12 (2001) 1341.

[9] Saleh, H., Hamideen, M., Al-Hwaiti, M., and Al-Kharoof, S., Jordan J. Phys., 11 (3) (2018) 193.

[10] Ababneh, E., Al-Amarat, S., Okoor, S., Imran, M., & Dababneh, S., Jordan J. Phys., 15(2), (2022) 149.

[11] Ababneh, E., Alzoubi, H., Qbelat, A. S., & Al-Bashaish, S. R., Journal of Physics Communications, 8(10) (2024) 105001.

[12] Ababneh, E., Qbelat, A. S., Imran, M. M., Al-Bashaish, S. R., Okoor, S., Darabee, A., & Mousa, M. S., Physica Scripta, 99 (8) (2024) 085303

[13] Ababneh, E., Mubayed, N., Okoor, S., Al-Bashaish, S. R., Qbelat, A. S., Sulieman, M., & Ershaidat, N. M., Radiation Detection Technology and Methods, 9(1) (2025) 132-144.

[14] Al-Bashish, S., Ababneh, E., Mousa, M. S., Okoor, S., Hyasat, M., Nusir, M., ... & Dababneh, S., Radiation Detection Technology and Methods, 5(3) (2021) 409-420.

[15] IAEA (International Atomic Energy Agency), Guidelines for Radioelement Mapping Using Gamma Ray Spectrometry Data, Vienna: IAEA. (IAEA-TECDOC-1363), (2003).

[16] EG&G Ortec, Gamma Vision-32, "Gamma-ray Spectrum Analysis and MCA Emulator". (EG&G Instruments Inc. Oak Ridge, Tennessee, 1999).

[17] Gilmore, G., "Practical Gamma-ray Spectrometry", (John Wiley & Sons, Ltd, 2, 2008).

[18] Issa, S., Uosif, M., and Elsaman, R., Turkish J. Eng. Environ. Sci., 37 (2013) 109.

[19] Al-Hamarneh I., Dirasat, Pure Sci., 33 (1) (2006) 49.

[20] Beretka, J. and Mathew, P.J., Health Phys., 48 (1) (1985) 87.

[21] Thabayneh, K.M., Arab. J. Sci. Eng., 38 (2013) 201.

[22] Lyngkhoi, B. and Nongkynrih, P., Egypt. J. Basic Appl. Sci., 7 (1) (2020) 194.

[23] UNSCEAR, United Nations Scientific Committee on the Effect of Atomic Radiation, Report to the General Assembly, Annex A and B Vol. 1 (2000).

[24] EC (European Commission), Radiation Protection, (Directorate-General Environment, Nuclear Safety and Civil Protection: Luxembourg, Belgium, 112, 1999).

[25] Jose, A., Kumar, A.S., Govindarajan, K.N., and Manimaran, P., J. Med. Phys., 45 (3) (2020) 182.

[26] Vineethkumar, V., Akhil, R., Shimod, P.K., and Prakash, V., J. Radioanal. Nucl. Chem., 327 (2021) 189.

[27] Al-Jundi, J., Salah, W., Bawaaneh, M.S., and Afaneh, F., Radiat. Prot. Dosim., 118 (1) (2006) 93.

[28] Todorović, N., Bikit, I., Krmar, M., Mrđa, D., Hansman, J., Nikolov, J., Todorović, S., Forkapić, S., Jovančević, N., Bikit, K., and Mandić, L.J., Rom. J. Phys., 62 (2017) 817.

[29] Khatun, M.A., Ferdous, J., and Haque, M.M., J. Environ. Prot., 9 (10) (2018) 1034.

[30] Estokova, A., Singovszka, E.، and Vertal, M., Mater. Marian, 15 (2022) 6876.

[31] Uosif, M., Omer, M., Ali, N.A., El-Kamal, A.H., and Hefni, M.A., Int. J. Adv. Sci. Technol., 80 (2015) 19.

[32] Xinwei, L. and Xiaolan, Z., Radiat. Prot. Dosim., 128 (1) (2008) 77.

[33] Righi, S. and Bruzzi, L., J. Environ. Radioact., 88 (2) (2006) 158.

[34] Stoulos, S., Manolopoulou, M., and Papastefanou, C., J. Env. Rad., 69 (3) (2003) 225.

[35] Papaefthymiou, H. and Gouseti, O., Radiat. Meas., 43 (8) (2008) 1453.

[36] Matiullah, N.A. and Hussein, A.J.A., J. Environ. Radioact., 39 (1) (1998) 9.

[37] Awadallah, M.I. and Imran, M.M., Dirasat: Pure Sciences, 34 (1) (2007).